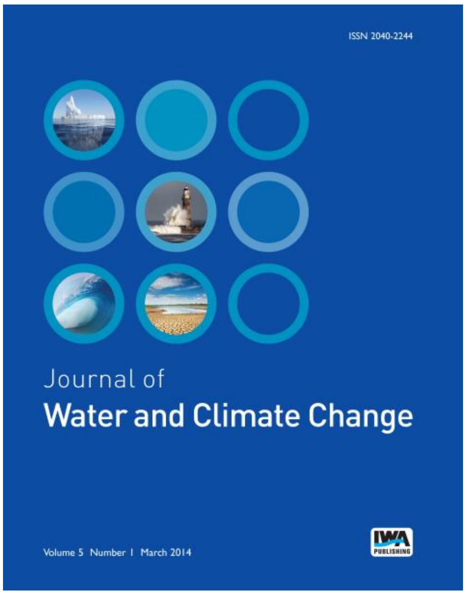
ISSN 2040-2244
Journal of
Water and Climate Change
Volume 5 Number 1 March 2014
IWA PUBLISHING

Analysis of rainfall trend and variability for agricultural water management in Awash River Basin, Ethiopia

Daniel Bekele, Tena Alamirew, Asfaw Kebede, Gete Zeleke and Assefa M. Melese

ABSTRACT

The national economy and food security of many sub-Saharan countries relies on rain-fed agriculture, hence the impact of rainfall variability is highly significant. The intent of this study is to characterize rainfall variability and trend in Awash River Basin for agricultural water management using standard rainfall statistical descriptors. Long-term climate data of 12 stations were analyzed. Onset and cessation dates, length of growing period (LGP) and probability of dry spell occurrences were analysed using INSTAT Plus software. The Mann–Kendall test and the Sen's slope method were used to assess the statistical significance of the trend. The results show high variability of rainfall (38–73%), LGP (30–38 days) and high probability of dry spell occurrence (up to 100%) during the *Belg* season (the short rainy season from March to May) compared with the *Kiremt* season (the main rainy season from June to September) in all stations. *Belg* season showed a non-significant decline trend in most of the stations, whereas the *Kiremt* season indicated the contrary. The finding also revealed that supplementary irrigation is vital, especially in the *Belg* season to cover up to 40% of the crop water requirement deficit.

Key words | Awash River Basin, Ethiopia, rainfall variability and trend, supplemental irrigation

Daniel Bekele
Ethiopian Institute of Agricultural Research,
Melkassa,
P.O. Box 436,
Adama,
Ethiopia

Tena Alamirew (corresponding author)
Gete Zeleke
Water and Land Resource Center,
P.O. Box 3880,
Addis Ababa,
Ethiopia
E-mail: *tena.a@wlrc-eth.org*

Asfaw Kebede
Institute of Technology, Haramaya University,
P.O. Box 138,
Dire Dawa,
Ethiopia

Assefa M. Melese
Department of Earth and the Environment,
Florida International University,
Miami,
FL 33199,
USA

INTRODUCTION

Sub-Saharan Africa is among the most vulnerable regions to climate changes (IPCC 2007; Kotir 2011). Even though the impact of climate change is vast, the changing pattern of precipitation deserves urgent and systematic attention as it affects food security in this part of the world (Dore 2005). The land phase hydrological system is mainly affected by precipitation, and changes in the precipitation pattern have direct impacts on water resources. A higher or lower rainfall or changes in its distribution would influence the water balance, and would alter the frequency of droughts and floods (Kumar *et al.* 2010). It is also noted that precipitation and temperature changes are not globally uniform. Regional variations can be much larger, and considerable spatial and temporal variations may exist between climatically different regions (Yue & Hashino 2003).

Trend analysis and variability in precipitation series have been investigated by many researchers throughout the world. The findings have indicated that there is a declining as well as an increasing trend of rainfall (Philandras *et al.* 2011) in the majority of Mediterranean regions with the exception of northern Africa, southern Italy and the western Iberian Peninsula. Kumar & Jain (2009) in Kashmir India, and Partal & Kahya (2006) in west and south Turkey found that there is a declining trend of rainfall. However, Taxak *et al.* (2014) in the Wainganga basin of central India and Osborn *et al.* (2000) in different regions of the UK reported significant increasing trends in annual rainfall. Many studies on rainfall revealed that the African continent exhibits higher inter-annual and intra-seasonal rainfall variability (Challinor *et al.* 2007; Cooper *et al.* 2009; 2011; Rosell

doi: 10.2166/wcc.2016.044

2011). There is also an emerging consensus that Eastern Africa, particularly Ethiopia, is one of the most susceptible regions regarding the impacts of climate variability and change (Slingo *et al.* 2005; Challinor *et al.* 2007; Thornton *et al.* 2011).

Different studies were conducted to assess the variability and trend of rainfall in different parts of Ethiopia. Mengistu *et al.* (2014) in the Upper Blue Nile River Basin of Ethiopia, Kassie *et al.* (2013) in the Central Rift Valley of Ethiopia, Wing *et al.* (2008) in several parts of Ethiopia, Woldeamlak & Conway (2007) in drought prone areas of Amhara region, Seleshi & Zanke (2004) in central, northern, and northwestern Ethiopia, Conway *et al.* (2004) in the central Ethiopian highlands and Conway (2000) in the northeastern Ethiopian highlands agreed that there is no significant and clear trend in the annual rainfall pattern. Contrasting results of annual and seasonal rainfall trend in some parts of the country were also reported (Seleshi & Zanke 2004; Degefu & Bewket 2014).

Natural rainfall is the main source of water for crop production as irrigation covers only 5% of the cultivated land in Ethiopia (Awulachew *et al.* 2010). Hagos *et al.* (2009) examined the impact of rainfall variability on the Ethiopian economy, and found that rainfall variability in the country led to a production deficit (20%) and increases the poverty rates (25%), which costs the economy over one-third of its growth potential. Rainfall variability and associated droughts have historically been major causes of food shortages and famines (Pankhurst & Johnson 1988).

The Ethiopian highlands are characterized by a bi-modal rainfall pattern (Shanko & Camberlin 1998; Kassie *et al.* 2013). The *Belg* rainfall (the short rainy season from March to May) is caused by humid easterly and south-easterly winds from the Indian Ocean, whereas the *Kiremt* rainfall (the main rainy season from June to September) is a result of convergence in low-pressure systems associated with the Inter Tropical Convergence Zone (Conway 2000; Seleshi & Zanke 2004). The migration of ITCZ is sensitive to variations in Indian Ocean sea surface temperatures that vary from year to year, influencing the characteristics of the season in the region as well as episodes of El Niño Southern Oscillation and La Niña (Dessu & Melesse 2013). Understanding the characteristics and variability of Ethiopia's principal monsoon rainy season (*Kiremt*) and the early (*Belg*) rains is vital for ensuring the food supply and well-being of the nation which, unfortunately, has been ravaged by severe and recurrent drought for many years (Segele & Lamb 2005).

Efforts are being made to understand rainfall trend, variability and characteristics of the seasons, not only because of their significance for agriculture but also for their role in energy production, drinking water supply, and management and utilization of resources. Understanding the variability, trend and characteristics of the growing season is, therefore, crucial for planning and designing appropriate adaptation strategies in the basin. Out of the 12 river basins in Ethiopia, the Awash River Basin is the most important, intensively utilized and environmentally vulnerable (Kinfe 1999; Edossa *et al.* 2010). The river provides consistent irrigation water to a large and productive agricultural area. It is also used for generating hydropower energy and the fresh water supply for big towns and cities like Addis Ababa and Adama, and many other small towns along its course. The basin thus has an important contribution towards the sustainable development of the national economy. The objectives of this study were to explore the spatial and temporal characteristics of rainfall, and to analyze the variability and trends of annual and seasonal rainfall for agricultural water management in the Awash River Basin.

MATERIALS AND METHODS

The study area

The Awash River Basin covers a total area of about 110,000 km^2. It lies within 7°53′47″ to 12°07′20″ N latitude and 37°56′23″ to 42°57′21″ E longitude (Figure 1). The river rises to an altitude of about 3,000 m above sea level (m.a.s.l.) near Ginchi town west of Addis Ababa in Ethiopia, and flows along the rift valley for the rest of its course to Lake Abe on the border with the Djibouti Republic, at an altitude of about 250 m.a.s.l. The total length of the main course is about 1,200 km. The Awash River Basin has been divided into three distinct zones: the Upper Basin, Middle Basin, and Lower Basin, on the basis of various inter-related factors such as location, altitude, climate, topography, agricultural development, inhabitants, administrative boundaries, etc. (Kinfe 1999). The mean annual precipitation of the basin

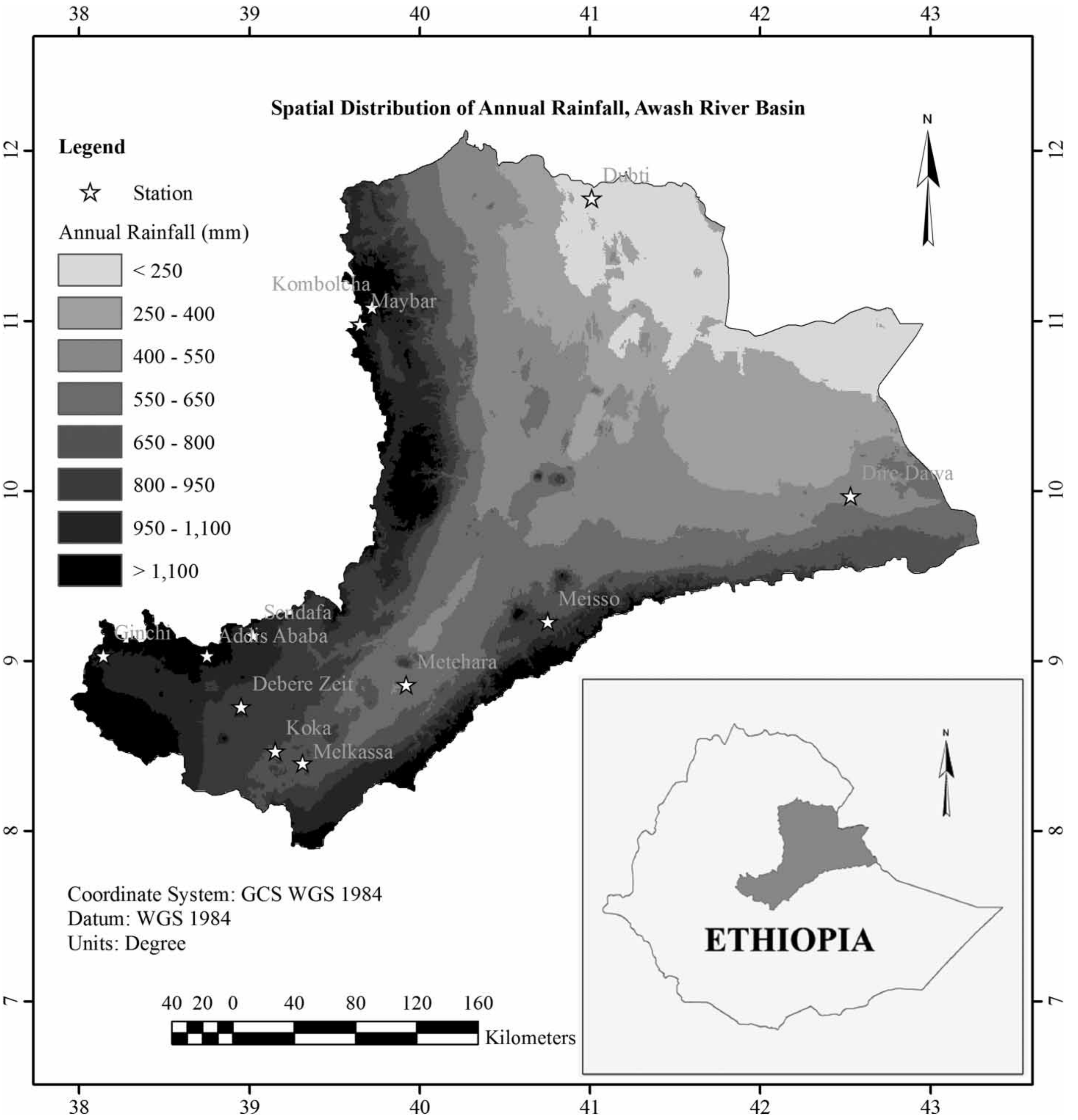

Figure 1 | Location map of the Awash River Basin with spatial distribution of annual rainfall based on World Clim Global climate data (Hijmans *et al.* 2005).

varies from about 1,600 mm, in the highlands north east of Addis Ababa, to 160 mm, in the northern point of the basin. Rainfall distribution is mostly bimodal in the Middle and Lower Awash and unimodal in the Upper Awash (Edossa *et al.* 2010).

Data sources

Daily rainfall and temperature data of 20 stations were obtained from the National Meteorological Agency, Ethiopian Institute of Agricultural Research and Water and

Land Resources Center of Ethiopia. Twelve stations for rainfall data and four stations for minimum and maximum temperatures from different agro-ecology were selected, which have relatively long periods of data records (at least 30 years) and have no more than 10% missing values based on Rosell (2011) and Seleshi & Zanke (2004), except Dubti station, which has only 26 years' data (Table 1).

Data quality control

Outlier detection

The Tukey fence was used to screen the outliers greater than a threshold value that can affect the detection of inhomogeneity (Ngongondo *et al.* 2011) (Equation (1)). The data range is represented as:

$$[Q_1 - 1.5 \times IQR, Q_3 + 1.5 \times IQR] \tag{1}$$

where Q_1 and Q_3 are the lower and upper quartile points, respectively and IQR is the interquartile range. Values outside the Tukey fence are considered as outliers. In this study, such outliers were set to a limit value corresponding to $1.5 \times \text{IQR}$.

Homogeneity test

The cumulative deviation test was used to detect inhomogeneity in the meteorological time series data (Sahin & Kerem 2010; Ngongondo *et al.* 2011). Buishand (1982) noted that tests for homogeneity can be based on the adjusted partial sums or cumulative deviations from the mean, and it is given by Equation (2):

$$S_o* = 0 \quad and \quad S_k* = \sum_{i=1}^{k} (y_i - \bar{y}), \ k = 1, \ldots, n \tag{2}$$

The term S_k* is the partial sum of the given series. If there is no significant change in the mean, the difference between y_i and $\bar{y}$ will fluctuate around zero (y_i is the annual series and $\bar{y}$ is the mean). The significance of the change in the mean is calculated with 'rescaled adjusted range' R, which is the difference between the maximum and the minimum of the S_k* values scaled by the sample standard deviation as:

$$R = \left(\max\ S_k* - \min\ S_k*\right)/SD \quad 0 \le k \le n \tag{3}$$

The critical values for the test-statistic ($R/\sqrt{n}$) is recommended by Buishand (1982) and for $n = 30$, and 5 and 10% probability levels, its values are 1.5 and 1.4, respectively.

Table 1 | Rainfall and temperature data of the selected stations at the Awash River Basin and arranged according to their alphabetical order

				Rainfall data		**Temperature**	
Station	**Latitude (°N)**	**Longitude (°E)**	**Elevation (m)**	**Periods**	**Missing (%)**	**Periods**	**Missing (%)**
Addis Ababa	9.03	38.75	2,354	1951–2012	0.4		
DebereZeit	8.73	38.95	1,900	1951–2012	3.9		
Dire Dawa	9.97	42.53	1,180	1953–2012	1.3	1980–2012	8.4
Dubti	11.72	41.01	376	1986–2011	9.5		
Ginchi	9.03	38.14	2,272	1968–2012	4.4		
Koka	8.47	39.15	1,618	1982–2012	9.8		
Kombolcha	11.08	39.72	1,840	1958–2012	2.3	1985–2013	2.6
Maybar	10.98	39.65	2,140	1981–2013	10.0	1986–2014	10.0
Meisso	9.23	40.75	1,400	1968–2012	8.0		
Melkassa	8.40	39.31	1,540	1977–2012	0.2	1980–2012	9.8
Metehara	8.86	39.92	944	1984–2013	5.2		
Sendafa	9.15	39.02	2,550	1965–2008	7.7		

Data pre-processing

Data were captured with Microsoft Excel 2000 spreadsheets following the days of year entry format. To prepare the series for further analyses, the missing values were generated following the first order Markov chain model using INSTAT Plus (v3. 37) software (Stern *et al.* 2006). Then, the generated data were checked for their physical representativeness of the respective sites. INSTAT Plus software was also used to summarize the daily data into annual, monthly and seasonal totals and to analyse the onset and cessation of the rainy season and length of growing period (LGP).

Data analysis

Trend analysis

Mann–Kendall's and Sen's Slope Estimator tests were used for trend tests. Mann–Kendall's test is a non-parametric method, which is less sensitive to outliers and tests for a trend in a time series without specifying whether the trend is linear or non-linear (Partal & Kahya 2006). The initial value of the Z test statistics S is assumed to be zero, implying no trend. If a data value from a later time period is found to be greater than the data value from an earlier time period, then S is incremented by one. On the other hand, if the data value from the later time period is lower than that of the earlier period, the Z test statistics S is reduced by one. The overall result of all increments and decrements provides the final S value, which lies between −1 and +1. The null hypothesis of the Z test is no change has occurred during the time (no trend). Whereas the alternative hypothesis of the Z test is a significant change has occurred over the time.

The Mann–Kendall test statistics are given as follows (Salmi *et al.* 2002; Longobardi & Villani 2009):

$$S = \sum_{k=1}^{n-1} \sum_{j=k+1}^{n} \operatorname{sgn}(X_j - X_k) \tag{4}$$

$S =$ any integer between $-n\left(\frac{n-1}{2}\right)$ and $n\left(\frac{n-1}{2}\right)$, X_j and X_k are sequential time series values, n is the number of data in the set, sgn (X_j–X_k) is the sign function and is given as:

$$\operatorname{Sgn}(X_j - X_k) = \begin{cases} 1 & \text{if } (\mathrm{X_j} - X_k) > 0 \\ 0 & \text{if } (\mathrm{X_j} - X_k) = 0 \\ -1 & \text{if } (\mathrm{X_j} - X_k) < 0 \end{cases} \tag{5}$$

It is also assumed that for $n \geq 8$, the S test statistics are normally distributed with a mean value of zero and variance is calculated using Equation (6):

$$\sigma^2 = \frac{n(n-1)(2n+5)}{18} \tag{6}$$

From this, the standardized test statistics, Z, is calculated using the following relations:

$$Z = \begin{cases} \dfrac{S-1}{\sigma} & \text{if S} > 0 \\ 0 & \text{if } S = 0 \\ \dfrac{S+1}{\sigma} & \text{if S} < 0 \end{cases} \tag{7}$$

The decision to either reject or accept the null hypothesis is then made by comparing the calculated Z with the critical value at a chosen level of significance.

Sen's Slope Estimator is also a non-parametric test by which the true slope (change per year) of a trend is estimated (Salmi *et al.* 2002). Sen's test is used when the trend is assumed to be linear, i.e.

$$f(t) = Qt + B \tag{8}$$

where $f(t) =$ increasing or decreasing function of time, i.e. the trend $Q =$ the slope and $B =$ intercept (constant).

The slope of each data pair Q_i is calculated as:

$$Q_i = \frac{x_j - x_k}{j - k} \tag{9}$$

where $j > k$ and, if there is n number of x_j in the time series, we get as many as $N = \frac{n(n-1)}{2}$ slope estimates of Q_i.

Then the values of Q_i are ranked from small to large; the median of which is the Sen's slope (Q):

$$\mathrm{Q} = \begin{cases} Q_{\left[\frac{(N+1)}{2}\right]} & \text{if N is odd} \\ \frac{1}{2}\left(Q_{\left[\frac{N}{2}\right]} + Q_{\left[\frac{(N+2)}{2}\right]}\right) & \text{if N is even} \end{cases} \tag{10}$$

Onset and cessation of the growing season

According to Stern *et al.* (2006), the start of the rainy season can be defined as the first occurrence of at least '*X*' mm of rainfall totalled over '*t*' consecutive days. This potential start can be a false start if an event *F* occurs afterwards, where *F* is defined as a dry spell of '*n*' or more days in the next '*m*' days. Accordingly, the earliest start of the growing season is the first occasion when the rainfall accumulated within a 3-day period is 20 mm or more. Various authors used similar criteria in assessing the start of the growing season (Barron *et al.* 2003; Stern *et al.* 2006; Kassie *et al.* 2013). The risk of crop failure of early planting was assessed by adding a caveat, i.e. the potential starting date of the growing season that was not followed by a dry spell of 10 or more days in the first 30 days after planting. The end of the growing season is mainly dictated by stored soil water and its availability to the crop after the rainfall stops. Stern *et al.* (2006) defined the end of the season as the first date on which soil water is depleted and reaches zero.

Dry spell analysis

Daily rainfall data for each meteorological station were fitted to a simple Markov chain model. This was used to assess the chance of rain by assuming that the previous day is dry, i.e. the chance that a dry spell continues, and also the chance of rain by assuming that the previous day is rainy, i.e. the chance that a rain spell continues, which is known as a Markov chain (Stern *et al.* 2006; Stern & Cooper 2011). The probability of dry spell lengths of 5, 7, 10 and 15 days during the growing season were determined from the Markov chain model to obtain an overview of dry spell risks during the crop growing period (Kassie *et al.* 2013).

Rainfall variability

The Standardized Anomaly Index (SAI), Precipitation Concentration Index (PCI) and Coefficient of Variation (CV) were used as descriptors of rainfall variability (Woldeamlak & Conway 2007). SAI was calculated as the difference between the annual total of a particular year and the long term average rainfall records divided by the standard deviation of the long term data. This index, which is used to examine the nature of the trends, also helps us to determine the dry and wet years in the record. Its formula is given as:

$$Z = \frac{(x - \mu)}{\delta} \tag{11}$$

where Z is the standardized rainfall anomaly; x is the annual rainfall total of a particular year; μ is mean annual rainfall over a period of observation; and σ is the standard deviation of annual rainfall over the period of observation.

PCI was analysed using Equation (12) (De Luis *et al.* 2000):

$$PCI = \sum_{i=1}^{12} p_i^2 / \left(\sum_{i=1}^{12} p_i \right)^2 \times 100 \tag{12}$$

where P_i is the rainfall amount of the ith month. PCI values below 10 indicate uniform monthly rainfall distribution; values between 11 and 20 indicate high concentrations of monthly rainfall distribution; and values of 21 and above indicate very high concentrations of monthly rainfall distribution (De Luis *et al.* 2000; Woldeamlak & Conway 2007).

CV is a unit-less normalized measure of dispersion of a probability distribution. It expresses the standard deviation as a fraction of the mean and is useful when interest is in the size of variation relative to the size of the observation. In comparing different years of rainfalls with different means, the CV is a more useful basis of comparison than the standard deviation. It is expressed as the ratio of the standard deviation to the mean (Araya & Stroosnijder 2011):

$$CV = \left[\frac{S}{X} \right] \times 100 \tag{13}$$

where CV is the coefficient of variation; X is the average long-term rainfall and S is the standard deviation of rainfall. The CV was used to compare the long-term variation of wet season rainfall to that of individual years.

Seasonal deficit in crop water requirement

Seasonal crop water requirements for major crops in the basin from planting to maturity were calculated using the CROPWAT 8 model (Allen *et al.* 1998):

$$ET_C = K_C \times ET_O \tag{14}$$

where ET_c is the crop water requirement (mm); K_c is the crop coefficient and ET_o is reference evapotranspiration (mm). ET_o was computed using the FAO Penman–Monteith method from long term minimum and maximum temperature data using the CROPWAT 8 model.

The irrigation water requirement was computed as:

$$IWR = ET_C - ER \tag{15}$$

where IWR is supplemental irrigation water requirement (mm) and ER is the effective rainfall (mm). Effective rainfall was calculated based on an empirical formula developed by FAO to estimate dependable rainfall, the combined effect of dependable rainfall (80% probability of exceedance), and losses due to runoff and deep percolation.

RESULTS AND DISCUSSION

Characteristics of the rainfall

The mean annual rainfall distribution across the 12 stations in Awash River Basin varies from 209.7 mm in Dubti to 1,186.8 mm in Addis Ababa (Table 2). However, many of the stations in the Basin receive less than 900 mm rainfall per annum. The annual weighted average rainfall of the stations is 853.1 mm with 22.7% CV. With the exception of Koka (CV% >30), most of the stations show moderate variation in annual rainfall (CV% <30) (Charles *et al.* 2005).

Kiremt season (June–September) received 66% of the mean annual rainfall, whereas *Belg* season (March–May) received 23%. Sendafa (870.6 mm) and Ginchi (258.4 mm) stations registered high *Kiremt* and *Belg* season rainfall in the basin respectively, while Dubti registered the minimum rainfall and no *Belg* season (Figure 2). All stations showed a high coefficient of variation (CV% >30) for *Belg* season rainfall. However, apart from Koka, all stations showed moderate variation in *Kiremt* season rainfall (CV% <30). The forward and retreat pace of the African sector of the inter-tropical convergence zone (ITCZ) and their ending and beginning times vary annually, causing most of the inter-annual variability in rainfall over Ethiopia (Seleshi & Zanke 2004). Moreover, according to Shanko & Camberlin (1998), *Belg* rainfall is more influenced by the cyclonic activity. The PCI value is more than 11% for all of the stations and highlights the seasonality in rainfall distribution (Woldeamlak & Conway 2007) (Table 2).

The SAI calculated for the station mean of annual, *Kiremt* and *Belg* season rainfall indicates that 50.8, 49.5 and 58.8% of the years during the past 33 years exhibited negative anomalies

Table 2 | Mean rainfall (mm), CV (%) and PCI result for annual, *Kiremt* and *Belg* rainfall in the Awash River Basin

	Annual		***Kiremt* season**		***Belg* season**		
Station	**Mean**	**CV**	**Mean**	**CV**	**Mean**	**CV**	**PCI**
Addis Ababa	1,186.8	13.3	845.9	15.0	231.2	42.5	14.9
DebereZeit	856.3	23.1	633.9	22.8	151.5	54.6	17.0
Dire Dawa	605.2	23.2	306.7	32.4	208.3	49.8	12.6
Dubti	209.7	27.5	119.1	44.7	63.5	76.8	16.9
Ginchi	1,142.2	17.4	744.2	17.5	258.4	42.3	13.3
Koka	810.6	47.1	582.1	49.7	154.7	72.7	17.0
Kombolcha	1,049.1	15.4	676.6	21.2	229.1	38.4	16.1
Maybar	1,135.8	25.5	718.9	28.9	233.8	48.9	15.6
Meisso	769.0	22.0	410.0	30.9	242.7	52.5	12.2
Melkassa	823.7	18.5	554.2	19.8	163.1	48.2	14.9
Metehara	491.2	17.9	302.7	23.6	123.7	49.4	14.9
Sendafa	1,158.1	21.0	870.6	20.5	201.9	53.6	18.7
Mean	**853.1**	**22.7**	**563.7**	**27.3**	**188.5**	**52.5**	**15.3**

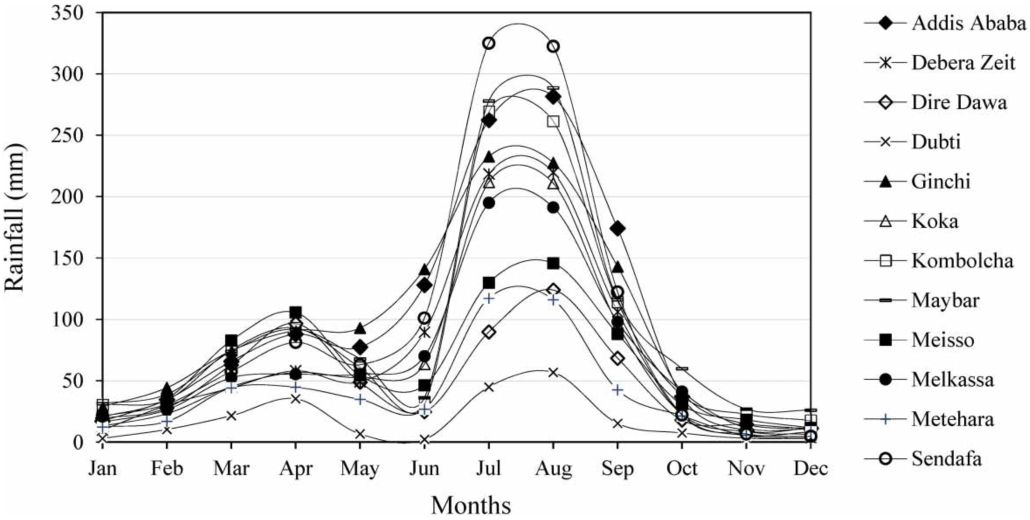

Figure 2 | Monthly rainfall distribution of Awash River Basin at the selected station.

respectively and the frequency of negative anomalies increased during recent years (Table 3). The results indicate that the stations in the basin have experienced more dry seasons (less than the long-term mean rainfall) than wet seasons (greater than long-term mean rainfall), especially in *Belg* rainfall. The probability of dry season occurrence for *Belg* rainfall is much higher than for the *Kiremt* season. The development of numerous tropical depressions in the Southwest Indian Ocean (SWIO) is associated with significant circulation anomalies in both the lower and upper troposphere, extending to the Northern Hemisphere. In such years, the enhancement of the northern Hadley cell results in a reduced low-level moisture advection towards East Africa, and stronger (weaker) upper easterlies (westerlies) over the equator and northeastern Africa. This creates unfavorable conditions for convective activity in Ethiopia, thus leading to below-normal *Belg* rainfall (Shanko & Camberlin 1998).

Table 3 | Percentage of positive and negative standardized anomaly index (SAI) result for annual, *Kiremt* and *Belg* rainfall of the selected stations in Awash River Basin, Ethiopia

	Standardized anomaly index (%)					
	Annual		***Kiremt* season**		***Belg* season**	
Station	**SAI (+)**	**SAI (−)**	**SAI (+)**	**SAI (−)**	**SAI (+)**	**SAI (−)**
Addis Ababa	42.4	57.6	51.5	48.5	39.4	60.6
DebereZeit	54.5	45.5	57.6	42.4	36.4	63.6
Dire Dawa	42.4	57.6	48.5	51.5	39.4	60.6
Dubti	50.0	50.0	38.5	61.5	*NBS*	*NBS*
Ginchi	42.4	57.6	48.5	51.5	42.4	57.6
Koka	54.8	45.2	51.6	48.4	35.5	64.5
Kombolcha	48.5	51.5	51.5	48.5	48.5	51.5
Maybar	53.1	46.9	48.4	51.6	38.7	61.3
Meisso	51.5	48.5	57.6	42.4	45.5	54.5
Melkassa	45.5	54.5	54.5	45.5	48.5	51.5
Metehara	53.3	46.7	50.0	50.0	43.3	56.7
Sendafa	51.7	48.3	48.3	51.7	37.9	62.1
Mean	**49.2**	**50.8**	**50.5**	**49.5**	**42.9**	**57.1**

NBS: No *Belg* season.

Trends of rainfall in Awash River Basin

The annual and *Belg* rainfall indicated a decline in trend for eight and seven stations respectively even though it is not statistically significant except for Addis Ababa, Koka and Meisso where reduction in the annual rainfall trend is statistically significant ($P < 0.05$) (Table 4). However, Dire Dawa registered a significant increment of *Belg* season rainfall in the basin. The *Kiremt* season rainfall shows an increasing trend in eight stations out of 12, Addis Ababa, Koka and Melkassa show statistically significant trends ($P < 0.05$) (Figure 3). Generally, the direction and magnitude of the seasonal rainfall trend was not uniform throughout different stations.

Table 4 | Mann–Kendall (Z) and Sen's slope (Q) trend test (mm/year) result for the annual and *Kiremt* and *Belg* rainfall of the selected stations in the Awash River Basin, Ethiopia. Bold values indicate a significance of $P < 0.05$

	Annual trend			***Kiremt* trend**			***Belg* trend**		
Station	**Z**	**Q**	***P*-value**	**Z**	**Q**	***P*-value**	**Z**	**Q**	***P*-value**
Addis Ababa	1.77	2.12	**0.045**	2.76	2.78	0.006	– 0.05	– 0.02	0.983
DebereZeit	– 0.70	– 0.84	0.527	– 1.11	– 1.20	0.258	0.49	0.24	0.676
Dire Dawa	0.77	0.69	0.240	– 0.94	– 0.61	0.407	2.19	1.34	**0.035**
Dubti	– 1.81	– 3.13	0.065	0.79	0.75	0.522	*NBS*	*NBS*	*NBS*
Ginchi	– 1.26	– 2.72	0.337	– 0.64	– 1.01	0.473	– 0.58	– 0.63	0.929
Koka	2.45	19.31	**0.029**	3.43	17.02	0.005	0.51	1.27	0.907
Kombolcha	– 0.25	– 0.25	0.815	1.67	2.15	0.110	– 0.01	– 0.001	0.700
Maybar	– 0.41	– 2.38	0.942	0.99	4.02	0.277	– 2.11	– 4.26	0.124
Meisso	– 2.24	– 4.52	**0.013**	– 0.90	– 1.15	0.416	– 1.54	– 1.78	0.322
Melkassa	2.79	6.33	0.130	2.63	4.88	0.016	0.56	0.87	0.706
Metehara	– 0.64	– 1.15	0.539	0.00	0.02	0.824	– 1.53	– 1.91	0.172
Sendafa	– 0.60	– 1.03	0.304	0.28	0.64	0.899	– 0.99	– 1.03	0.249

NBS: No Belg season.

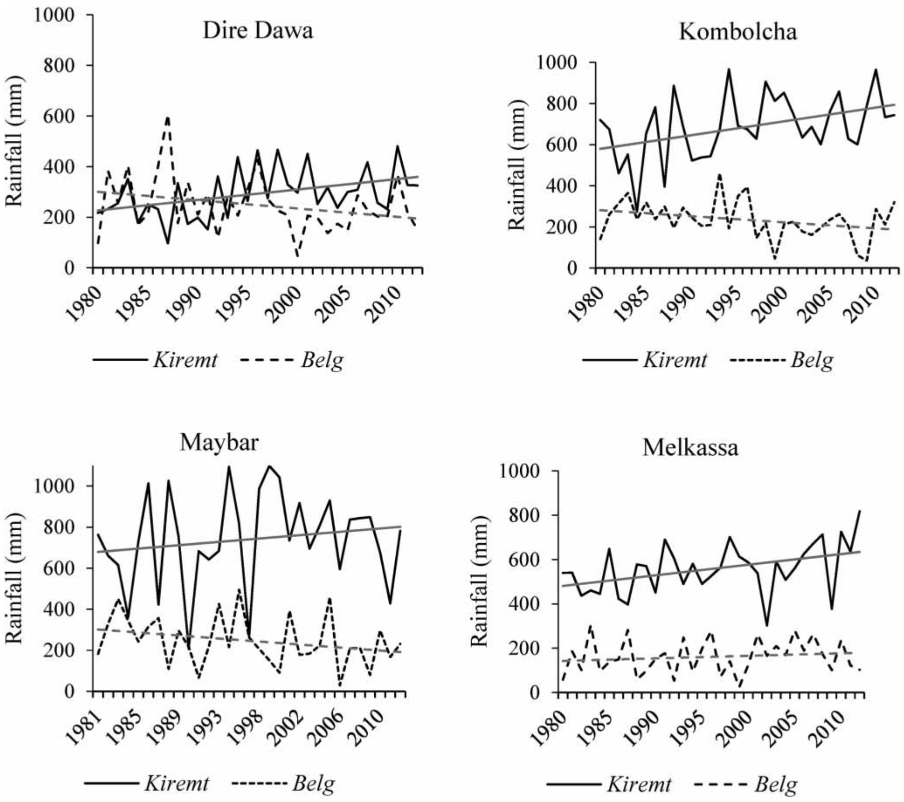

Figure 3 | *Kiremt* and *Belg* rainfall trend for selected stations representing the major agroecologies of the basin.

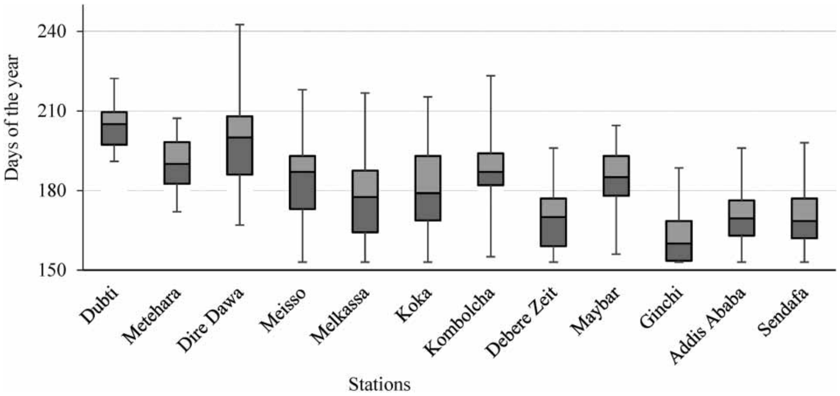

Figure 4 | Onset date of *Kiremt* growing season in the Awash River Basin arranged based on increasing order of stations' altitude.

Characteristics of the growing season

Start and end of the growing season

The mean potential onset date of the *Kiremt* growing season ranged from Julian day number 159 to 211 (i.e. 7 June to 29 July), while the corresponding value for the *Belg* growing season is 63 to 144 (i.e. 3 March to 22 May) (Figures 4 and 5). The standard deviation for the start of the season (SOS) of the *Kiremt* and *Belg* growing seasons ranged from 7.8 to 17.6 and 16.9 to 31.8 days respectively. The results revealed a higher inter-annual variability of SOS observed in the *Belg* season than the *Kiremt* season. Shanko & Camberlin (1998) described that *Belg* rainfall is much more influenced by the cyclonic activity than *Kiremt* rainfall, which occurs outside the cyclonic season of the SWIO. The results exhibit a serious uncertainty of crop production for the *Belg* season due to inter-annual rainfall variability in the SOS. The possibility of delayed or earlier SOS for the *Belg* season is enormous compared to the *Kiremt* season.

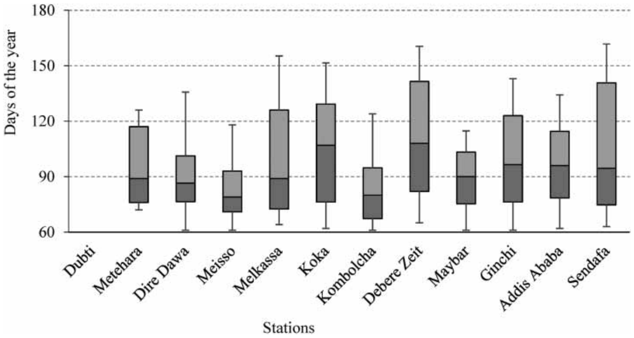

Figure 5 | Onset date of *Belg* growing season in the Awash River Basin based on increasing order of stations' altitude, with no *Belg* season for Dubti.

The boxes in Figures 4–9 indicate the lower and upper quartiles. The solid line within the box is the median and the whiskers indicate minimum and maximum values observed.

The mean potential cessation date of the *Kiremt* and *Belg* growing season in the Awash River Basin ranged from Julian day number 262 to 299 (i.e. 17 September to 25 October) and 152 to 222 (i.e. 30 May to 17 June) respectively (Figures 5 and 6). The standard deviation for the cessation of the season of the *Kiremt* and *Belg* growing season ranged from 1 to 14.8 and 0.4 to 7 days respectively. The standard deviation of cessation dates is less than the onset dates in all stations of the basin. Segele & Lamb (2005) revealed that the range of temporal variability about the mean onset date is large and depends on geographical region. They also found that *Kiremt* onset is positively correlated with the preceding December–February sea-surface temperatures (SST) over the equatorial central and eastern Pacific Ocean and *Kiremt* cessation correlates poorly with SST in the tropical Atlantic and Pacific basins, but more strongly (positively) with SST in the western Indian Ocean and Arabian Sea.

LGP

The mean potential LGP of the *Kiremt* and *Belg* growing season ranged from 35 to 127 days and 0 to 82 days respectively (Figures 8 and 9). The standard deviation of LGP for the *Kiremt* growing season ranged from 9.9 to 31.9 days, while the standard deviation of LGP for the *Belg* growing

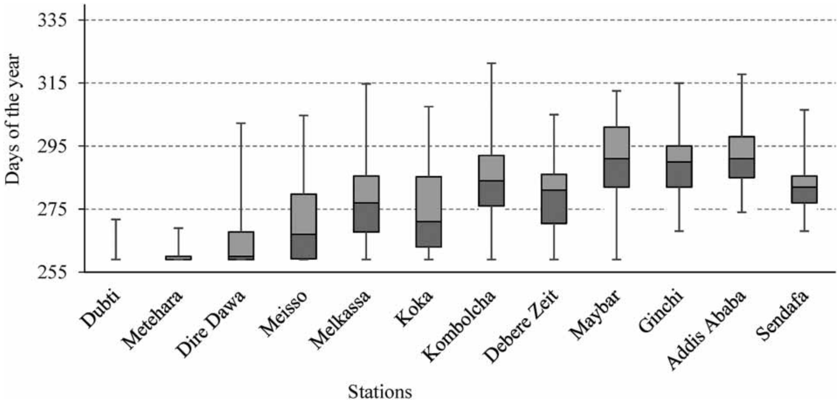

Figure 6 | Cessation date of *Kiremt* growing season in the Awash River Basin based on increasing order of stations' altitude.

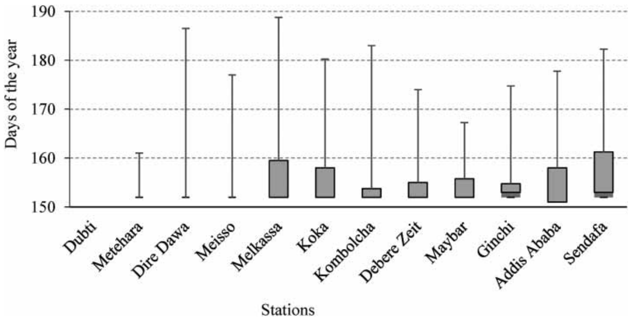

Figure 7 | Cessation date of *Belg* growing season in the Awash River Basin based on increasing order of stations' altitude, with no *Belg* season for Dubti.

season ranged from 29.7 to 37.3 days. The results revealed high inter-annual variability of LGP in the *Belg* season compared to the *Kiremt* season because of high inter-annual variability in the onset and cessation date for the *Belg* season. Delayed onset and/or early cessation resulted in a shorter growing period, and this shows the serious uncertainty and risk for the *Belg* season crop production.

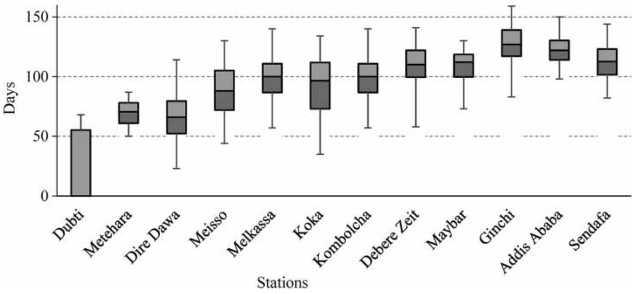

Figure 8 | LGP of *Kiremt* season in the Awash River Basin based on increasing order of stations' altitude.

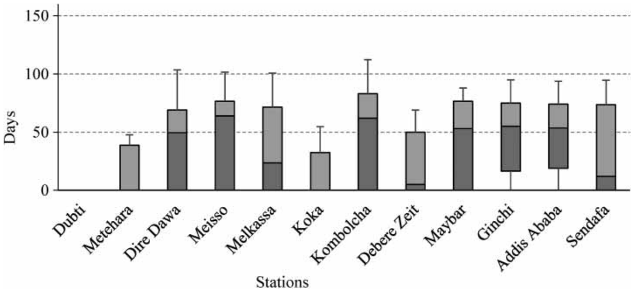

Figure 9 | LGP of *Belg* season in the Awash River Basin based on increasing order of stations altitude, with no *Belg* season for Dubti.

Trend of the growing season

The LGP for the *Belg* season indicated a decline in trend for all stations except Koka, which shows a statistically significant increment ($P < 0.05$). The probable reason as to why the variability is not statistically significant, for a declining trend, may be attributed to the high inter annual and inter seasonal variability of the data. However, the LGP for *Kiremt* shows an increasing trend in nine stations out of 12, and Koka station shows a highly significant increment ($P < 0.01$) (Table 5). The possible reason is that most of the stations registered an increasing rainfall trend during the *Kiremt* season.

Dry spells during the growing season

For all stations, the probability of occurrence of longer dry spells is less than 0.3 in March, decreasing to 0 from the middle to the end of June, and increasing again after the

Table 5 | Mann–Kendall (Z) and Sen's slope (Q) trend test (day/year) result for the LGP of the selected stations in Awash River Basin, Ethiopia. Bold values indicate a significance of $P < 0.05$

	***Kiremt* LGP trend**			***Belg* LGP trend**		
Station	**Z**	**Q**	***P*-value**	**Z**	**Q**	***P*-value**
Addis Ababa	0.80	0.08	0.457	– 0.57	– 0.08	0.692
DebereZeit	1.15	0.15	0.317	– 0.45	– 0.17	0.569
Dire Dawa	0.96	0.16	0.312	– 0.24	0.00	0.676
Dubti	– 0.41	0.00	0.664	*NBS*	*NBS*	*NBS*
Ginchi	0.00	0.00	0.769	– 0.79	– 0.43	0.908
Koka	3.77	1.96	**0.000**	0.74	0.00	**0.030**
Kombolcha	0.07	0.00	0.635	– 0.14	0.00	0.991
Maybar	0.99	0.40	0.281	– 0.78	– 0.19	0.355
Meisso	0.42	0.07	0.668	– 0.94	– 0.02	0.439
Melkassa	0.71	0.23	0.446	– 0.62	0.00	0.567
Metehara	– 0.21	– 0.05	0.914	– 1.41	0.00	0.251
Sendafa	1.17	0.25	0.512	– 0.51	0.00	0.605

NBS: No *Belg* season.

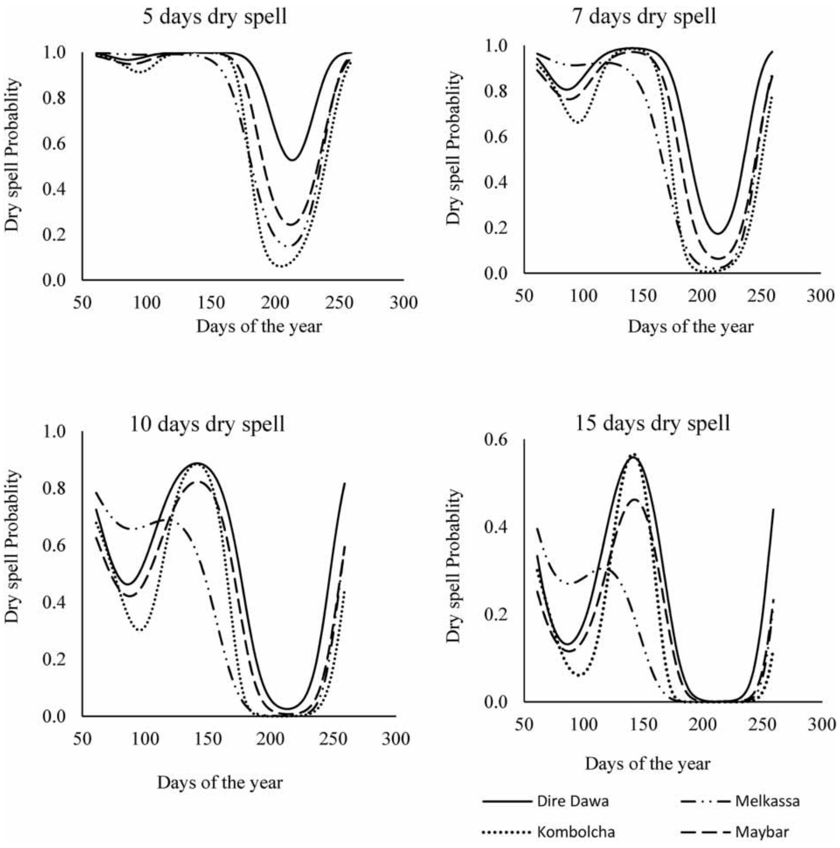

Figure 10 | Probability of dry spells longer than 5, 7, 10 and 15 days' length during the growing season for selected stations representing the major agroecologies of the basin.

end of August. All dry spell probability curves converge to their minimum during the peak rain season and increase again around September, signaling the end of the growing season (Figure 10). The results also revealed that the probability of the occurrence of a dry spell (shorter or longer) is higher in Dire Dawa and lower in Kombolcha, from the selected stations. In general, the *Belg* has a much higher probability of dry spells than the *Kiremt*. The increased probability of dry spells at all the stations in late August and thereafter might be related to the southward shift of the ITCZ (Araya & Stroosnijder 2011). Segele & Lamb (2005) verified that long and consecutive dry spells were strongly related to a major downturn in dew point, abnormally high temperatures, and easterly winds throughout the troposphere beneath a weak tropical easterly jet.

Seasonal deficit in crop water requirement

The crop water requirement simulation results showed that supplementary irrigation is vital in both seasons to avoid yield reduction and crop failure. The *Belg* season needs more supplementary irrigation than the *Kiremt* season, except for Dire Dawa station, and supplementary irrigation is needed more at the end of the two growing seasons even though the amount varies from station to station (Table 6). May and September are the most important months of the growing season, when flowering and yield formation take place and the crops are more sensitive to water stress. It is also possible to harvest sufficient runoff, especially in the *Kiremt* season in July and August, to be used as a supplementary irrigation when rainfall starts to decline (Araya & Stroosnijder 2011).

Table 6 | Effective rainfall (mm), Seasonal supplementary irrigation requirements (mm) and the monthly irrigation requirement (mm) for onion and maize in selected stations of the Awash River Basin

Crop	Unit	Dire Dawa	Kombolcha	Maybar	Melkassa
Onion	Crop water requirement (mm)	441.0	425.0	323.4	460.9
	Effective rainfall (mm)	100.7	113.3	115.7	69.8
	Total irrigation requirement (mm)	340.3	311.7	207.7	391.1
	March (mm)	82.0	68.3	29.3	94.6
	April (mm)	95.3	91.6	57.3	133.8
	May (mm)	162.7	151.8	120.7	162.7
Maize	Crop water requirement (mm)	522.0	485.2	391.1	454.2
	Effective rainfall (mm)	159.0	455.5	489.7	349.8
	Total irrigation requirement (mm)	362.9	29.7	0	104.4
	June (mm)	50.1	13.4	0	19.4
	July (mm)	102.3	0	0	7.3
	August (mm)	110.1	2.3	0	26.8
	September (mm)	100.2	14.0	0	50.8

CONCLUSIONS AND RECOMMENDATIONS

In conclusion, higher variations of rainfall existed in the *Belg* season than in the *Kiremt* season in all stations, even though *Kiremt* rainfall contributed the highest percentage of rainfall in the Basin. The *Belg* season rainfall and LGP show a declining pattern in most of the selected stations, although it is not statically significant. However, the *Kiremt* season rainfall and growing period indicate a non-significant increment in several stations. In general, the direction and magnitude of the seasonal rainfall and LGP trend performed using the Mann–Kendall test and the Sen's slope method was not uniform throughout the different stations. Higher inconsistencies in onset date, cessation date and LGP occurred in the *Belg* season than the *Kiremt* season. Besides, the variation of cessation dates is less than for onset dates in both seasons. The probability of occurrence of longer dry spells in the *Belg* season is much higher than in the *Kiremt* season all over the basin. To overcome the seasonal moisture deficit, supplementary irrigation is vital in both seasons to avoid yield reduction and crop failure for the majority of the stations. This is specifically critical in the mid and low altitude areas. Moreover, most of the supplementary irrigation is needed for the *Belg* season and for the end month of both growing seasons. Excess rainfall for harvesting is available in July and August in much of the basin. This excess water has a huge potential to ensure good crop establishment during the short rainy season (*Belg*), and can be used to ensure proper crop seed establishment. Moreover, if rain stops early during the main rain season, the water harvested in July and August can assist proper crop maturity. Moreover, given the high uncertainties in *Belg* season crop production, farmers need to be provided with an enhanced forecast service.

REFERENCES

Allen, R. G., Pereira, L. S., Raes, D. & Smith, M. 1998 *Crop Evapotranspiration (Guidelines for Computing Crop Water Requirements)*. FAO Irrigation and Drainage Paper No. 56. FAO, Rome, Italy.

Araya, A. & Stroosnijder, L. 2011 Assessing drought risk and irrigation need in northern Ethiopia. *Agric. For. Meteorol.* **151**, 425–436.

Awulachew, S. B., Erkossa, T. & Namara, R. E. 2010 *Irrigation Potential in Ethiopia: Constraints and Opportunities for Enhancing the System.* International Water Management Institute, Colombo, Sri Lanka.

Barron, J., Rockstrom, J., Gichuki, F. & Hatibu, N. 2003 Dry spell analysis and maize yields for two semi-arid locations in east Africa. *Agric. For. Meteorol.* **117**, 23–37.

Buishand, T. A. 1982 Some methods for testing the homogeneity of rainfall records. *J. Hydrol.* **58**, 11–27.

Challinor, A., Wheeler, T., Garforth, C., Craufurd, P. & Kassam, A. 2007 Assessing the vulnerability of food crop systems in Africa to climate change. *Clim. Change* **83**, 381–399.

Charles, V. J., Ellen, M. D., Pamela, A. G. & Carmen, R. 2005 Geospatial indicators of emerging water stress: an application to Africa. *AMBIO A J. Hum. Environ.* **34**, 230–236.

Conway, D. 2000 Some aspects of climate variability in the north east Ethiopian highlands – Wollo and Tigray. *SINET Ethiop. J. Sci.* **23**, 139–161.

Conway, D., Mould, C. & Bewket, W. 2004 Over one century of rainfall and temperature observations in Addis Ababa, Ethiopia. *Int. J. Climatol.* **91**, 77–91.

Cooper, P., Rao, K. P. C., Singh, P., Dimes, J., Traore, P. S., Rao, K., Dixit, P. & Twomlow, S. J. 2009 Farming with current and future climate risk: advancing a 'Hypothesis of Hope' for rainfed agriculture in the semi-arid tropics. *J. SAT Agric. Res.* **7**, 1–19.

Cooper, P. J. M., Coe, R. & Stern, R. D. 2011 Assessing and addressing climate-induced risk in Sub-Saharan rainfed agriculture. *Exp. Agric.* **47**, 179–410.

Degefu, M. & Bewket, W. 2014 Variability and trends in rainfall amount and extreme event indices in the Omo-Ghibe river basin, Ethiopia. *Reg. Environ. Change* **14**, 799–810.

De Luis, M., Raventos, J., Gonzalez-Hidalgo, C., Sanchez, J. R. & Cortina, J. 2000 Spatial analysis of rainfall trends in the region of Valencia (East Spain). *Int. J. Climatol.* **20**, 1451–1469.

Dessu, S. B. & Melesse, A. M. 2013 Impact and uncertainties of climate change on the hydrology of the Mara river basin, Kenya/Tanzania. *Hydrol. Process.* **27**, 2973–2986.

Dore, M. H. I. 2005 Climate change and changes in global precipitation patterns: what do we know? *Environ. Int.* **31**, 1167–1181.

Edossa, D. C., Babel, M. S. & Gupta, A. Das. 2010 Drought analysis in the Awash river basin, Ethiopia. *Water Resour. Manage.* **24**, 1441–1460.

Hagos, F., Makombe, G., Namara, R. & Awulachew, S. 2009 *Importance of Irrigated Agriculture to the Ethiopian Economy: Capturing the Direct Net Benefits of Irrigation.* International Water Management Institute, Colombo, Sri Lanka.

Hijmans, R. J., Cameron, S. E., Parra, J. L., Jones, P. G. & Jarvis, A. 2005 Very high resolution interpolated climate surfaces for global land areas. *Int. J. Climatol.* **25**, 1965–1978.

IPCC 2007 *Climate Change 2007: Impacts, Adaptation and Vulnerability: Contribution of Working Group II to the Fourth Assessment Report of the Intergovernmental Panel, Genebra, Suíça.* Cambridge University Press, New York, USA.

Kassie, B. T., Rötter, R. P., Hengsdijk, H., Asseng, S., Van Ittersum, M. K., Kahiluoto, H. & Van Keulen, H. 2013 Climate variability and change in the Central Rift Valley of Ethiopia: challenges for rainfed crop production. *J. Agric. Sci.* **152**, 58–74.

Kinfe, H. 1999 Impact of climate change on the water resources of Awash river basin, Ethiopia. *Clim. Res.* **12**, 91–96.

Kotir, J. H. 2011 Climate change and variability in Sub-Saharan Africa: a review of current and future trends and impacts on agriculture and food security. *Environ. Dev. Sustainability* **13**, 587–605.

Kumar, V. & Jain, S. K. 2009 Trends in seasonal and annual rainfall and rainy days in Kashmir Valley in the last century. *Quat. Int.* **212**, 64–69.

Kumar, V., Jain, S. K. & Singh, Y. 2010 Analysis of long-term rainfall trends in India. *Hydrol. Sci. J.* **55**, 484–496.

Longobardi, A. & Villani, P. 2009 Trend analysis of annual and seasonal rainfall time series in the Mediterranean area. *Int. J. Climatol.* **30**, 1538–1546.

Mengistu, D., Bewketa, W. & Lalb, R. 2014 Recent spatiotemporal temperature and rainfall variability and trends over the Upper Blue Nile river basin, Ethiopia. *Int. J. Clim.* **34**, 2278–2292.

Ngongondo, C., Xu, C. Y., Gottschalk, L. & Alemaw, B. 2011 Evaluation of spatial and temporal characteristics of rainfall in Malawi: a case of data scarce region. *Theor. Appl. Climatol.* **106**, 79–93.

Osborn, T. J., Hulme, M., Jones, P. D. & Basnett, T. A. 2000 Observed trends in the daily intensity of United Kingdom precipitation. *Int. J. Climatol.* **20**, 347–364.

Pankhurst, R. & Johnson, D. H. 1988 *The Ecology of Survival: Case Studies from Northeast African History.* Lester Crook Academic Publishing, I.B. Tauris, London, pp. 47–72.

Partal, T. & Kahya, E. 2006 Trend analysis in Turkish precipitation data. *Hydrol. Process.* **20**, 2011–2026.

Philandras, C. M., Nastos, P. T., Kapsomenakis, J., Douvis, K. C., Tselioudis, G. & Zerefos, C. S. 2011 Long term precipitation trends and variability within the Mediterranean region. *Nat. Hazards Earth Syst. Sci.* **11**, 3235–3250.

Rosell, S. 2011 Regional perspective on rainfall change and variability in the central highlands of Ethiopia, 1978–2007. *Appl. Geogr.* **31**, 329–338.

Sahin, S. & Kerem, C. H. 2010 Homogeneity analysis of Turkish meteorological data set. *Hydrol. Process.* **24**, 981–992.

Salmi, T., Määttä, A., Anttila, P., Ruoho-Airola, T. & Amnell, T. 2002 *Detecting trends of annual values of atmospheric* *pollutants by the Mann-Kendall test and Sen's slope estimates –the Excel template application MAKESENS*. Finnish Meteorological Institute, Helsinki, Finland.

Segele, Z. T. & Lamb, P. J. 2005 Characterization and variability of Kiremt rainy season over Ethiopia. *Meteorol. Atmos. Phys.* **89**, 153–180.

Seleshi, Y. & Zanke, U. 2004 Recent changes in rainfall and rainy days in Ethiopia. *Int. J. Climatol.* **983**, 973–983.

Shanko, D. & Camberlin, P. 1998 The effects of the southwest Indian ocean tropical cyclones on Ethiopian drought. *Int. J. Climatol.* **18**, 1373–1388.

Slingo, J. M., Challinor, A. J., Hoskins, B. J. & Wheeler, T. R. 2005 Introduction: food crops in a changing climate. *Phil. Trans. R Soc. Lond. B Biol. Sci.* **360**, 1983–1989.

Stern, R. D. & Cooper, P. J. M. 2011 Assessing climate risk and climate change using rainfall data – a case study from Zambia. *Exp. Agric.* **47**, 241–266.

Stern, R., Rijks, D., Dale, I. & Knock, J. 2006 *INSTAT Climatic Guide*. Statistical Service Centre, University of Reading, UK.

Taxak, A. K., Murumkar, A. R. & Arya, D. S. 2014 Long term spatial and temporal rainfall trends and homogeneity analysis in Wainganga basin, Central India. *Weather Clim. Extremes* **4**, 50–61.

Thornton, P. K., Jones, P. G., Ericksen, P. J. & Challinor, A. J. 2011 Agriculture and food systems in sub-Saharan Africa in a 4 °C+ world. *Phil. Trans. A Math. Phys. Eng. Sci.* **369**, 117–136.

Wing, H. C., Senay, G. B. & Singha, A. 2008 Trends and spatial distribution of annual and seasonal rainfall in Ethiopia. *Int. J. Climatol.* **1734**, 1723–1734.

Woldeamlak, B. & Conway, D. 2007 A note on the temporal and spatial variability of rainfall in the drought-prone Amhara region of Ethiopia. *Int. J. Climatol.* **1477**, 1467–1477.

Yue, S. & Hashino, M. 2003 Long-term trends of annual and monthly precipitation in Japan. *Am. Water Resour. Assoc.* **39**, 587–596.

First received 5 March 2016; accepted in revised form 24 June 2016. Available online 20 August 2016